Ellipse Detection on Images Using Conic Power of Two Points

Min Liu
liu66@purdue.edu

Bodi Yuan
bodiyuan@berkeley.edu

Jing Bai
baijing_nun@163.com

Purdue University
West Lafayette, IN, USA

University of California, Berkeley
Berkeley, CA, USA

Beifang University of Nationalities
Yinchuan, China

Abstract

Elliptical features are evident in abundance, in a wide variety of digital images. Much of these features carry useful statistical and geometrical information that can be explored for a broad range of real-world applications. In this paper, we propose and analyze a novel method which is independent of the popular Hough transform or random sample consensus approaches, to detect elliptical features in a digital image. Our method is based upon the circle power theorem and its extension to conics. The key idea is to transform an image into several power ratio histograms that record the distribution of power ratios computed from some reference point pairs. We show that the peaks in a power ratio histograms provide strong evidence for the existence of ellipses. Peak verification based on the parallel chord property together with multi histogram cross validation increase the confidence of an identified peak. Experiments over several synthetic as well as natural images validate the efficacy of the proposed method in terms of its accuracy and robustness.

1 Introduction

Object detection is a necessary intermediate stage and long-standing goal in many computer vision paradigms. Among the simplest features treated in object detection, circles and their perspective projections, ellipses are moderately complex and frequently encountered. Much of them carry within themselves useful information that can be explored for a broad range of real-world applications such as product inspection and quality control [6, 34, 44], spatial surveying and exploration [35, 36, 37], surveillance and security [21, 45], cell segmentation [23] and character reconstruction [38]. Industrial applications are increasingly challenging the limits of circular and elliptical feature extraction by demanding high-resolution imagery at full frame rate. Real-time and robust detection of ellipses (circle as well as its special case) on images will be focus of this paper.

1.1 Related work

Current ellipse detection methods for images can be broadly divided into three categories: voting/clustering methods, optimization methods and edge following methods. Methods in

the first group include Hough Transform(HT) [15] and its variants [4, 8, 22, 24, 25, 27, 29, 32, 40, 45], RANSAC [9, 14], fuzzy logic [12, 19], and Kalman filtering [31]. These methods map one or sets of points to the parameter space to detect ellipses through accumulator voting or clustering. Voting/clustering methods are robust to outliers, but in general, they are computationally expensive due to the fact that an ellipse is specified by five parameters. And thus voting or clustering in a five-dimension parameter space are typically required which is the major threshold for most of voting/clustering methods.

The second group of methods, which includes least-square fitting [1, 3, 17, 26, 33], genetic algorithm [23, 41], and point set registration algorithm [2], formalize ellipse detection as an optimization problem. They fit selected data points to ellipses while optimizing a specific error metric. Although optimization methods are generally accurate and faster than voting/clustering methods, their performance depends heavily on pre-processing steps such as pixel segmentation or grouping. These methods are also limited by the fact that they can fit only one primitive at a time, and in most cases, they will yield false or missing detections when the subset contains more than 50% outliers [11]. Hence they are more suitable for a later stage curve fitting after a subset of points corresponding to a hypothetical ellipse has been roughly identified and separated.

The third category, edge following methods [10, 16, 18, 28, 30], explicitly exploits the connectivity between edge pixels to detect ellipses. Local geometric information such as tangent [16], internal angle and convexity [10, 18], curvature [28], Zernike moment [30] are used for tracking the small segments along a potential ellipse. Edge following method combined with HT is also proposed [7]. The main limitation with these methods is that local geometric information is very sensitive to noise, intersection and occlusion, and a bias estimation in a local point may propagate into the subsequent stage of the contour tracking, resulting in an incorrect group decision. These methods, therefore, run the relative high risk of false detection.

indeed one of the most widely used techniques for ellipse detection.Thanks to the voting mechanism, HT-based method is less sensitive to noises, shape disconnectedness and occlusions. However, it suffers meanwhile the disadvantage of massive requirements of computations and memory storage. Therefore, HT-based methods for ellipse detection presented in literature usually involve some sort of decomposition, or alternatively, sub-sampling in the parameter space. Decomposition methods usually work by detecting the centers first using geometric properties of ellipses such as diameter bisection[32], parallel chord[22], or chord-tangent[20, 43, 45]. And then the rest of three parameters are calculated employing a standard voting process or least square fitting. The Randomized Hough transform (RHT)[27, 29, 39, 40] is a popular sub-sampling method which alleviates the problems of standard HT using a many-to-one converging mapping, but its performance degrades as the number of ellipses in the image increases [27].

In [42], a circle detector has been developed based on the circle power histogram. According to the circle power theorem, the edge pixels on a circle share the same circle powers with respect to an arbitrary reference point on the image. In this paper, we extended the circle power theorem into conics, and showed that the ratios between two conic powers calculated from two arbitrary reference points always remain constant. A power ratio histogram based ellipse detector is proposed based on the theorem of conic power of two points. our method detects the presence of candidate ellipses by identifying signal peaks in a power ratio histogram. Cross validation among multiple reference points and mid-chord validation are further proposed to increase the robustness of the proposed method. By using geometric properties of circles and ellipses, the proposed method levels the advantages of the voting

and clustering methods and avoids their extensive resources consumption.

2   Theoretic Background

Circle Power of a Point Theorem: Consider a circle O and a point P in the plane where P is not on the circle. Draw a line through P that intersects the circle in two places, then the product of the length from P to the first point of intersection and the length from P to the second point of intersection is constant for any choice of a line through P that intersects the circle. This constant is called the power of point P. For example, in Figure 1(a), $PX^2 = PA_1 \cdot PB_1 = PA_2 \cdot PB_2 = \cdots == PA_i \cdot PB_i$. The theorem still holds when P is inside the circle, or if A_k and B_k coincide (as is the case with X). The circle power of a point theorem can be extended into conics as follows.
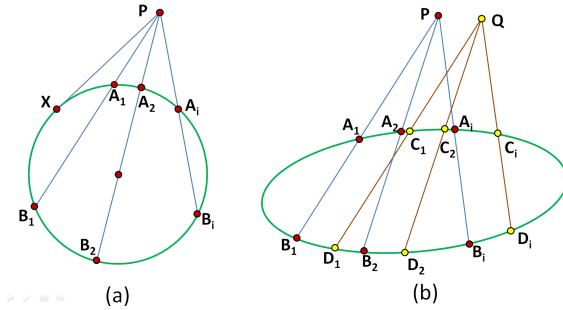

Figure 1: Extend the circle power of a point into the conic power of two points. (a) Circle powers to a point are $PX^2, PA_1 \cdot PB_1, PA_2 \cdot PB_2$ or $PA_i \cdot PB_i$, and (b) Ellipse power ratios of two points are $\frac{PA_1 \cdot PB_1}{QC_1 \cdot QD_1}, \frac{PA_2 \cdot PB_2}{QC_2 \cdot QD_2}$, or $\frac{PA_i \cdot PB_i}{QC_i \cdot QD_i}$.

Conic Power of two Point Theorem: Consider a conic curve O and two point P and Q in the plane where P and Q are not on the conic. Draw a pair of parallel lines through P and Q that intersects the conic in two places respectively, then the ratio between the power of point P to the power of point Q is constant for any choice of a set of parallel lines through P and Q that both intersect the conic. This constant is called the power ratio of two points P and Q. For example, in Figure 1(b),

$$\frac{PA_1 \cdot PB_1}{QC_1 \cdot QD_1} = \frac{PA_2 \cdot PB_2}{QC_2 \cdot QD_2} = \cdots = \frac{PA_i \cdot PB_i}{QC_i \cdot QD_i} \tag{1}$$

The theorem still holds when P and Q are inside the conic, or if A_k and B_k coincide. The proof to this theorem is given in Appendix A.

Parallel chord property of conics: *The bisecting line of any two parallel chords of a conic curve is incident to the center of the conic curve.* A graphical illustration to the parallel chord property of elliptical curves is given in Fig. 2, where A_iB_i and C_iD_i are two parallel chords of the ellipse and M_iN_i is their bisecting line. According to the parallel chord property, M_iN_i will always pass through the center of the given ellipse. The formal proof
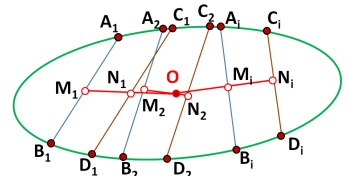

Figure 2: Illustration of the Parallel chord property of ellipse

to the parallel chord property can be found in Appendix B.

3   Ellipse Detection Using Conic Power

Given an input image I, the method first identifies its edge map E using Canny's operator [6] or other alternatives. It then separates E into a set of disconnected components E_i. These two steps are pre-processing steps designed to obtain a refined subset of edge pixels for further detection. For each decomposed edge map component E_i, the propose detector starts by calculating a reference triplet $R = \{R_1, R_2, R_3\}$, and they will be used pairwise as the reference points for conic power ratio calculation. Our method then builds three power ratio histograms for each component. Peaks in a power ratio histogram are the strong indicators of potential elliptic features in an image. The method detects initial set of peaks in generated power ratio histograms using peak detection signal method. However, those initially detected peaks are possibly accompanied with spurious pixels due to system noise and randomness, they need to be verified and trimmed carefully before the final ellipses fitting is conducted. The proposed method verifies the detected peaks from highest to lowest, based on a mid-chord verification process and a cross-validation process. After the two-steps of verification, the peaks will have high confidence level of being true ellipse indicators and will be fitted with ellipses at the final step.

3.1   Constructing power ratio histograms

A power ratio histogram is the distribution of power ratios calculated from scanning an edge map component using a set of rotational and parallel scanning lines passing through two reference points. Conic power of two points theorem suggests that among all the power ratios of any 4-tuple intersection points, the occurrence rate for the power ratios corresponding to the conic curves located in the image, should be relatively high. This can be illustrated by the synthetic example shown in Fig.3. Notice that there is a prominent peak in the power ratio histogram constructed which is an indicator for the ellipse presented in the given image.

The two reference points can be theoretically located anywhere on the image. But practically, one may expect that the rotating scan lines intersect the potential ellipses at as many pixels as possible. The strategy of computing the reference triplet for a component E_i is as follows. (1) Calculate the centroid $\mathbf{c}_i$ of the component E_i. (2) Construct a regular triangle around $\mathbf{c}_i$, with a random slanted angle and side length of 0.08α, where α is the diagonal distance of the bounding box of E_i. (3) The three vertices are then used as the reference points, in a pairwise way to generate three power ratio histograms for further verification.
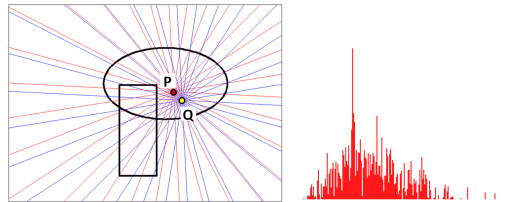

Figure 3: Illustration of the power ratio histogram construction given two reference points P and Q.

3.2 Peak detection and verification

Ideally, a power ratio histograms will present peaks for ellipses detection by using a simple absolute threshold strategy. But in practice, due to quantization errors and noises, the peaks on a power ratio histogram may be spread across the histogram and overlaid with spurious peaks. As the example shows in Fig.3, besides the highest peak, there are also some other spurious peaks which are irrelevant to any pattern in the image. We use the peak detection signal method proposed in [42] to identify all the relevant peaks while filtering out spurious ones. The idea is to apply a Gaussian filter to smooth the histogram first and then to use a zero crossing signal to located salient peaks.

Two separate verification processes are proposed to increase the robustness of the detected peak and the associated pixel sets to be fitted. The first verification process is **mid-chord verification** using the parallel chord property of conics. Given a peak Λ, mid-chord verification works as follows: (1) Get Λ's associated pixel set in the form of 4-tuples, draw the two parallel chords from each 4-tuple. (2) Draw the bisecting line segment (or mid-chords) for each pair of parallel chords. (3) Do a pairwise intersection computation to find out all the intersecting points among all the mid-chords. (4) Calculate the *main center* of the intersection points, filter out all the 4-tuples whose mid-chords do not pass through the *main center* within a predefined "mid-chord tolerance" ε_m. In the last step, the *main center* C is calculated as:

$$\mathsf{C} = \frac{\sum_{i=1}^{n} o_i^2 \times p_i}{\sum_{i=1}^{n} o_i^2} \tag{2}$$

where o_i is the occurrence of intersection point p_i. The squared occurrence term o_i^2 gives the intersection points with more occurrences larger weights so that the main center is expected to be located at the center of a dense cluster.

The second verification process, the **cross-validation**, validates each peak, from the highest to the lowest, across the three power ratio histograms. It relate a peak from a histogram to the peaks in the other two and validate the associated pixels. The process works as follows: (1) Locate the highest peak Λ among all unchecked peaks, get its associated pixel set $\wp(\Lambda)$. (2) Find the *nucleus* of Λ, or $\diamond(\Lambda)$, as a subset of $\wp(\Lambda)$, which is defined as $\diamond(\Lambda) = max\{\wp(\Lambda) \cap \wp(\Lambda_i) \cap \wp(\Lambda_j)\}$, where Λ, Λ_i and Λ_j are three peaks from different power ratio histograms and their intersection gives the largest subset of $\wp(\Lambda)$. (3) Repeat the previous 2 steps until all the peaks have been validated.

3.3 Curve fitting and parameter estimation

After the two processes of peak validation, the pixel set $\diamond(\Lambda)$ associated with each verified peak Λ could be a general conic, according to the conic power of two points theorem and the parallel chord property discussed in Section 2. In this paper, we handle only ellipse and its special case, circle. For other types of conics, we fit them as ellipses first and then use the geometric distance error to filter out non-elliptic features.

The general conic curve $F(\mathbf{a}, \mathbf{x}) = 0$ can be approached by minimizing the sum of squared algebraic distances $D_A(\mathbf{a}) = \sum_{i=1}^{N} F(\mathbf{a}, \mathbf{x}_i)^2$ of the curve to the N data point $x_i(i = 1, \cdots, N)$ in the pixel set in $\diamond(\Lambda)$. Here we adopted the ellipse-specific fitting method proposed in [17] so that all data will always return an ellipse. This is achieved by minimizing the above algebraic distance $D_A(\mathbf{a})$ subject to the constraint $4ac - b^2 = 1$.

Let the ellipse associated with $\diamond(\Lambda)$ be $\mathbb{E}$ and its algebraic coefficient obtained above be $\mathbf{a} = [a\ b\ c\ d\ e\ f]^T$. The geometric parameters $\{x_c, y_c, A, B, \theta\}$ of $\mathbb{E}$ are the center (x_c, y_c), the

major and minor axes (A, B) and the orientation angle θ, can they can all be calculated based on [3].

Non-elliptic features can then be filtered out if the number of points locating on the fitted ellipse is too few. Let the set of pixels located on a fitted ellipse $\mathbb{E}$ be $N_{\mathbb{E}}$. Then for a true ellipse on an image, the ratio between the size of $N_{\mathbb{E}}$ to the "mean radius" $(A+B)/2$ of the fitted ellipse should be larger than a pre-defined "existing rate threshold" R_e, i.e., $\frac{2|N_{\mathbb{E}}|}{(A+B)} \geq R_e$.

The number of pixels located on the obtained ellipse $N_{\mathbb{E}}$ can be computed based on the estimated geometric distance from an pixel x_i in $\Diamond(\Lambda)$ to the fitted $\mathbb{E}$. I.e.,

$$N_{\mathbb{E}} = |\{x_i| \frac{|dist(x_i, c) - r_\alpha|}{r_\alpha} \leq \varepsilon_l,\ x_i \in \Diamond(\Lambda)\}|, \tag{3}$$

where c is the center of the ellipse with coordinate (x_c, y_c), r_α is the directional radius of the ellipse in the direction of $\overrightarrow{cx_i}$ and ε_l is a predefined "locating threshold". r_α is calculated as follows.

$$\alpha = tan^{-1}\frac{y - y_c}{x - x_c} - \theta, \quad r_\alpha = \sqrt{(acos\alpha)^2 + (bsin\alpha)^2} \tag{4}$$

4   Experimental evaluation

The proposed algorithm has been tested through a series of experiments. All of them performed on an Intel CPU Core i7-3667U 2GHz processor with 4GB RAM. These experiments mainly address tasks such as: (1)Accuracy of ellipse location and shape discrimination on various images. (2) Multiple ellipse and circle detection capability. (3) Robustness under certain amount of imperfections such as deformations, occlusions, or noise.

Here are the parameter settings in our experiments: the number of the scanning lines N_s is related to the pixel size of the input image. For an image of $m \times n$ pixels, N_s is set as $m + n$. Note that the resolution of a power ratio histogram is set to 1 for simplicity. The peak denoising parameter σ is set to 3.3321. The selection of this parameter σ is based on the length estimation $1.1107n$ of digital line segments suggested in [13]. The mid-chord tolerance ε_m is set as 2.2214 for the same reason. The last two parameters: the existing rate threshold R_e and the locating threshold ε_l are two voting parameters which controls the errors a fitted ellipse can be tolerant for a point set. We set R_e as 1 in out experiments and ε_l is set as 10% empirically.

Test on synthetic images: The first experiments are conducted on a number of synthetic images of various sizes. Each image has been generated by drawing some randomly located ellipses. Those ellipses are possibly intersected with some other shapes or intersected to each other. Fig.4 gives three examples. The "synth1" image in Fig.4(a) contains two ellipses with different sizes and orientation. The two ellipses have been correctly detected. The special case circle detection capability is shown in Fig. 4(b). This "synth2" image consists of several intersected geometric shapes. The circle and the ellipse in it have been located precisely, demonstrating that the proposed ellipse detection method is capable of handling circles. The third testing example "synth3" (Fig. 4(c)) contains two intersected and overlaid ellipses, one of them is incomplete, and the proposed method has the capability to locate them separately as in one component.

Test on hand-sketched images: One of the main characteristics that our method confers is the capability to detect elliptical shapes deformed to a certain degree. This can be shown
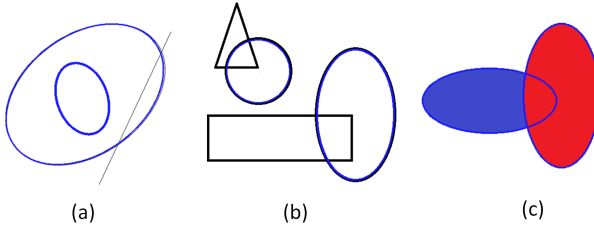
Figure 4: Experiment on some synthetic images. (a) , (b) and (c) show the original synthetic images named as "synth1","synth2" and "synth3" images, and their corresponding detected ellipses (or circles), as overlays on the original images.

when processing images such as those in Fig. 5. We can say that the system performance is adequate to both as it discriminates the hand-sketched ellipses and circles from other shapes and determines the best approximation for the desired elliptical or circular features.
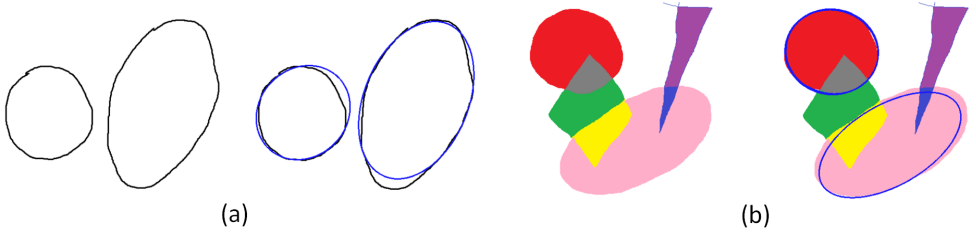

Figure 5: Experiment on hand-sketched images. (a) Sketch1 image and its ellipse detection result. (b) Sketch2 image and its corresponding ellipse detection result.

The observed robustness and flexibility of our method is due to the fact that the proposed method incorporates an imperfection tolerant mechanism through a smoothing and denoising step in a peak detection and verification process. The denoising step filters out some local deviations, while the peak verification step removes system errors linked to randomness and therefore, our method can efficiently handle imperfect and noisy ellipses while avoiding false positives.

Test on real life images: This experiment tests the efficacy of the proposed method on real-life images in which perfect ellipses (circles) are rarely found. Figure 6 shows seven representative examples from a number of test images. Among them, the "tea cup" image and the "manhole cover" image contain only a singe ellipse in each. The "glasses" image comprises two equal size ellipses while the traffic sign image comprises a set of multiple large and small ellipses. The "coin" image is a real-life image with multiple circles in it. The last two images, the "motorcycle" and the "big Ben" image are two examples with complex background and foreground. In all cases, it can be shown that the proposed method has been able to detect the ellipse's parameters correctly and the detection time is reasonably low for medium sized images (typically around 1-4s). We summarize our experimental results in Table 1.

From Table 1, it is also evident that the execution time of the proposed ellipse detector is dependent on the image size, the edge map size $|E|$ and the number of components $\sharp_c$ in it. Generally speaking, for a image of size $m \times n$ pixels, around $m + n$ rays are necessary

to be shot when constructing a power ratio histogram. For each power ratio histogram, it takes around $O(\frac{|E|}{\sharp_c})$ time to validate pixel-ray correspondence and a worst case $O((\frac{|E|}{m+n})^4)$ time complexity to construct a power ratio histogram. For the total $3\sharp_c$ power histograms, it requires the cross-validation and mid-chord verification for all the k detected peaks, taking time in a worst case complexity of $O(k\lg k + k\frac{|E|^2}{\sharp_c^2})$, where k is dependent on the number of ellipses in the image.

Figure 6: Test on real-life images: columns are tea cup, manhole cover, glasses, traffic sign, coin, motorcycle and big Ben images, and rows are the original inputs, the detected ellipses and circles overlaid on the input images. Note that all ellipses are rendered as blue while circle are rendered as red, and all images are scaled down to fit the page size.

Limitation: The proposed method has its limitation when handling ellipses with significant occlusion, of severe incompleteness or discontinuity, or of very small size; and it also relies on a good result of edge detection. For examples, several ellipses in the manhole cover in Fig.6 are not detected due to their small size or missing in edge detection. The occluded ellipses in the motorcycle image and the discontinuous ellipses in the big Ben example are missed for detection. When the ellipse is in those situations, our method may not work well since the chance of collecting enough intersection 4-tuples pixels for peak detection is relatively reduced.

Table 1: Experimental results after applying the proposed ellipse detector to images in Fig. 4, 5 and 6.

Image properties		$|E|^a$	$\sharp_c^b$	$T(ms)^c$
Name	Size			
synth1	412×425	3268	2	1768
synth2	512×512	4539	2	2902
synth3	500×398	1055	1	674
sketch1	512×512	3482	2	1320
sketch2	512×512	2809	1	1368
tea cup	512×434	2121	1	1506
manhole cover	266×200	1097	1	978
glasses	448×326	4255	2	1584
traffic sign	543×486	3935	4	3258
coin	423×354	5575	4	1513
motorcycle	576×360	8763	2	5508
big Ben	390×384	13428	1	4230

[a]$|E|$: The size of edge map after applying the edge detector.
[b]$\sharp_c$: The number of components in E.
[c]T: The execution time in ms.

5   Conclusion

This paper has presented an algorithm for elliptical shapes detection independent of the conventional Hough transform principles, or the RANSAC-based sampling and validation strategy. Based on the basic power theorem of circles and its extension to conics, the proposed method transforms the edge pixels on an image into power ratio histograms which denote the distribution of ratios between pairwise distance powers among all intersection points along different scan lines. Using the peaks in the power ratios histograms, the method can significantly reduce the search space for potential ellipses and improves detection accuracy. The mid-chord validation and cross validation further ensure the robustness of the method. It has been shown that the presented method is capable of detecting ellipses accurately in synthetic images and it can also reliably detect multiple circles and ellipses in hand-drawn or real-life images, even when the features are visible but present slight occlusions or discontinuities.

Acknowledgments

APPENDIX A Proof of the conic power of two points theorem

a general conic can be represented as an implicit second order polynomial:

$$F(\mathbf{a}, \mathbf{x}) = \mathbf{a} \cdot \mathbf{x} = ax^2 + bxy + cy^2 + dx + ey + f = 0 \tag{5}$$

where $\mathbf{a} = [a\ b\ c\ d\ e\ f]^T$ and $\mathbf{x} = [x^2\ xy\ y^2\ x\ y\ 1]^T$. $F(\mathbf{a}, \mathbf{x_P})$ is called the "algebraic distance" of a point $P(x_p, y_p)$ to the conic $F(\mathbf{a}, \mathbf{x}) = 0$. A line passing through point $P(x_p, y_p)$ with an angle α has the following parametric representation:

$$\left\{ \begin{array}{l} x = x_p + t cos\alpha \\ y = y_p + t sin\alpha \end{array} \right. \tag{6}$$

Substitute $\mathbf{x}$ in Eq. (13) with the above, we get:

$$a(x_p + tcos\alpha)^2 + b(x_p + tcos\alpha)(y_p + tsin\alpha) + \\ c(y_p + tsin\alpha)^2 + d(x_p + tcos\alpha) + e(y_p + tsin\alpha) + f = 0, \tag{7}$$

i.e.:

$$(acos^2\alpha + bcos\alpha sin\alpha + csin^2\alpha)t^2 + (2ax_p cos\alpha + bc_p sin\alpha + by_p cos\alpha + \\ 2cy_p sin\alpha + dcos\alpha + esin\alpha +)t + ax_p^2 + bx_p y_p + cy_p^2 + dx_p + ey_p + f = 0 \tag{8}$$

Consequently, the power of point P with respect to the conic is:

$$PA \cdot PB = t_1 t_2 = \frac{ax_p^2 + bx_p y_p + cy_p^2 + dx_p + ey_p + f}{acos^2\alpha + bcos\alpha sin\alpha + csin^2\alpha} = \frac{F(\mathbf{a}, \mathbf{x_P})}{acos^2\alpha + bcos\alpha sin\alpha + csin^2\alpha} \tag{9}$$

where t_1 and t_2 are the two roots of Eq. (16). Similarly,

$$QC \cdot QD = \frac{ax_q^2 + bx_q y_q + cy_q^2 + dx_q + ey_q + f}{a cos^2 \alpha + b cos \alpha sin \alpha + c sin^2 \alpha} = \frac{F(\mathbf{a}, \mathbf{x_Q})}{a cos^2 \alpha + b cos \alpha sin \alpha + c sin^2 \alpha} \quad (10)$$

Combining Eq. 9 and Eq. 10, we have,

$$\frac{PA \cdot PB}{QC \cdot QD} = \frac{F(\mathbf{a}, \mathbf{x_P})}{F(\mathbf{a}, \mathbf{x_Q})}$$

The algebraic distances of point P and Q are constant, therefore the ratio between two powers always remains constant.

APPENDIX B Proof of the parallel chord property

Let AB and CD be two arbitrary parallel chords with end points A, B, C, D on the conic $F(\mathbf{a}, \mathbf{x}) = 0$. The midpoints of the two chords are M and N respectively. Without losing generality, we can assume that the two parallel chords AB an CD are horizontal which are defined by the intersection segments of two horizontal lines $y = y_1$ and $y = y_2$ with the conic section $F(\mathbf{a}, \mathbf{x}) = 0$ (this assumption is valid since the ellipse can have arbitrary orientation). Then, the point A and B satisfy:

$$\left\{ \begin{array}{l} ax^2 + (by_1 + d)x + cy_1^2 + ey_1 + f = 0 \\ y = y_1 \end{array} \right. \quad (11)$$

Solving (9) for A and B yields the coordinates of mid point M : $(\frac{-by_1-d}{2a}, y_1)$. Similarly, the point C and D satisfy:

$$\left\{ \begin{array}{l} ax^2 + (by_2 + d)x + cy_2^2 + ey_2 + f = 0 \\ y = y_2 \end{array} \right. \quad (12)$$

and the coordinates of mid point N are $(\frac{-by_2-d}{2a}, y_2)$. The slope of line MN is then written as,

$$S_{MN} = \frac{-2a}{b} \quad (13)$$

The center coordinates (x_c, y_c) of a conic $F(\mathbf{a}, \mathbf{x}) = 0$ are [53]:

$$x_c = \frac{2cd - be}{b^2 - 4ac}, y_c = \frac{2ae - bd}{b^2 - 4ac}, \quad (14)$$

The slope of the line MO is,

$$S_{MO} = \frac{\frac{2ae-bd}{b^2-4ac} - y_1}{\frac{2cd-be}{b^2-4ac} + \frac{by_1+d}{2a}} = \frac{-2a}{b} \quad (15)$$

Hence, the three points M, N an O are collinear. This means line MN is incident to the center. The above expression $(20) - (24)$ are valid for any orientation of the xy-coordinate system relative to the conic section. Therefore, in general cases, parallel chord property holds for all chord directions.

References

[1] S. J. Ahn, W. Rauh, and H. J. Warnecke. Least-squares orthogonal distances fitting of circle, sphere, ellipse, hyperbola, and parabola. *Pattern Recognition*, 34(12):2283–2303, 2001.

[2] C. Arellano and R. Dahyot. Robust ellipse detection with gaussian mixture models. *Pattern Recognition*, 58:12–26, 2016.

[3] D. S. Barwick. Very fast best-fit circular and elliptical boundaries by chord data. *Pattern Analysis and Machine Intelligence, IEEE Transactions on*, 31(6):1147–1152, 2009.

[4] N. Bennett, R. Burridge, and N. Saito. A method to detect and characterize ellipses using the hough transform. *Pattern Analysis and Machine Intelligence, IEEE Transactions on*, 21(7):652–657, 1999.

[5] J. Canny. A computational approach to edge detection. *IEEE Transactions on Pattern Analysis and Machine Intelligence*, 8(6):679–698, June 1986. ISSN 0162-8828.

[6] C. Chatterjee and E. K.P. Chong. Efficient algorithms for finding the centers of conics and quadrics in noisy data. *Pattern Recognition*, 30(5):673–684, 1997.

[7] S. Chen, R. Xia, J. Zhao, Y. Chen, and M. Hu. A hybrid method for ellipse detection in industrial images. *Pattern Recognition*, 68:82–98, 2017.

[8] Y. C. Cheng. The distinctiveness of a curve in a parameterized neighborhood: Extraction and applications. *Pattern Analysis and Machine Intelligence, IEEE Transactions on*, 28(8):1215–1222, 2006.

[9] Y. C. Cheng and S. C. Lee. A new method for quadratic curve detection using k-ransac with accerleration techniques. *Pattern Recognition*, 28(5):663–682, 1995.

[10] A. Y. Chia, S. Rahardja, D. Rajan, and M. K. Leung. A split and merge based ellipse detector with self-correcting capability. *Image Processing, IEEE Transactions on*, 20 (7):1991–2006, 2011.

[11] G. Danuser and M. Stricker. Parametric model fitting: From inlier characterization to outlier detection. *Pattern Analysis and Machine Intelligence, IEEE Transactions on*, 20(3):263–280, 1998.

[12] R. Dave. Generalized fuzzy c-shells clustering and detection of circular and elliptical boundaries. *Pattern Recognition*, 25(7):713–721, 1992.

[13] L. Dorst and A. W. M. Smeulders. Length estimators for digitized contours. *Computer Vision, Graphics and Image Processing*, 40:311–333, 1987.

[14] F. Duan, L. Wang, and P. Guo. Ransac based ellipse detection with application to catadioptric camera calibration. *Neural Information Processing. Models and Applications*, 6444:525–532, 2010.

[15] R. O. Duda and P. E. Hart. Use of the hough transformation to detect lines and curves in pictures. *Communications of the ACM*, 15(1):11–15, 1972.

[16] H. Kitajima E. Kim, M. Haseyama. Fast and robust ellipse extraction from complicated images. In *IEEE International Conference on Information Technology and Applications (ICITA)*, pages 45–48, 2002.

[17] A. Fitzgibbon, M. Pilu, and R. B. Fisher. Direct least square fitting of ellipses. *Pattern Analysis and Machine Intelligence, IEEE Transactions on*, 21(5):477–480, 1999.

[18] M. Fornaciari, A., and R. Cucchiara. A fast and effective ellipse detector for embedded vision applications. *Pattern Recognition*, 47(11):3693–3708, 2014.

[19] H. Frigui and R. Krishnapuram. A comparison of fuzzy shell-clustering methods for the detection of ellipses. *Fuzzy Systems, IEEE Transactions on*, 4(2):193–199, 1996.

[20] N. Guil and E. L. Zapata. Lower order circle and ellipse hough transform. *Pattern Recognition*, 30(10):1729–1744, 1997.

[21] D. W. Hansen and Q. Ji. In the eye of the beholder: a survey of models for eyes and gaze. *Pattern Analysis and Machine Intelligence, IEEE Transactions on*, 32(3): 478–500, 2010.

[22] C. T. Ho and K. H. Chen. A fast ellipse/circle detector using geometric symmetry. *Pattern Recognition*, 28(1):117–124, 1995.

[23] N. Kharma, H. Moghnieh, J. Yao, Y. Guo, A. Abu-Baker, J. Laganiere, G. Rouleau, and M. Cheriet. Automatic segmentation of cells from microscopicimagery using ellipse detection. *Image Processing, IET*, 1(1):39–47, 2007.

[24] B. Kwon and D. Kang. Ellipse detection method based on the advanced three point algorithm. In *Frontiers of Computer Vision (FCV), 2015 21st Korea-Japan Joint Workshop on*, pages 1–5. IEEE, 2015.

[25] Y. Lei and K. C. Wong. Ellipse detection based on symmetry. *Pattern Recognition Letters*, 20(1):41–47, 1999.

[26] J. Liang, M. Zhang, D. Liu, X. Zeng, O. O. Jr, K. Zhao, Z. Li, and H. Liu. Robust ellipse fitting based on sparse combination of data points. *Image Processing, IEEE Transactions on*, 22(6):2207–2218, 2013.

[27] W. Lu and J. Tan. Detection of incomplete ellipse in images with strong noise by iterative randomized hough transform (irht). *Pattern Recognition*, 41(4):1268–1279, 2008.

[28] F. Mai, Y. S. Hung, H. Zhong, and W. F. Sze. A hierarchical approach for fast and robust ellipse extraction. *Pattern Recognition*, 41(8):2512ÂÍC2524, 2008.

[29] R. A. McLaughlin. Randomized hough transform: Improved ellipse detection with comparison. *Pattern Recognition Letters*, 19(3-4):299–305, 1998.

[30] R. A. McLaughlin and M. D. Alder. The hough transform versus the upwrite. *Pattern Analysis and Machine Intelligence, IEEE Transactions on*, 20(4):396–400, 1998.

[31] P. S. Nair and A. T. Saunders Jr. Fitting ellipses and predicting confidence envelopes using a bias corrected kalman filter. *Image and Vision Computing*, 8(1):37–41, 1990.

[32] P. S. Nair and A. T. Saunders Jr. Hough transform based ellipse detection algorithm. *Pattern Recognition Letters*, 17(7):777–784, 1996.

[33] P. L. Rosin. Further five-point fit ellipse fitting. *Graphical Models and Image Processing*, 61:245–259, 1999.

[34] D. Schleicher and B. Zagar. Image processing to estimate the ellipticity of steel coils using a concentric ellipse fitting algorithm. In *9th International Conference on Signal Processing, ICSPÂ ąÂŕ 08*, pages 884–890, 2008.

[35] S. Sellah and O. Nasraoui. An incremental hough transform for detecting ellipses in image data streams. In *20th IEEE International Conference on Tools with Artificial Intelligence, ICTAIÂ ąÂŕ08*, pages 45–48, 2008.

[36] A. Soetedjo and K. Yamada. Fast and robust traffic sign detection. In *IEEE International Conference on Systems, Man and Cybernetics*, pages 1341–1346, 2005.

[37] Y. Soh, J. Bae, D. Kim, and H. Kim. A new method for ellipse fitting in satellite images. In *Second International Conference on Intelligent Computation Technology and Automation, ICICTAÂ ąÂŕ09*, pages 502–506, 2009.

[38] S. T. Wong, H. Leung, and H. Ho-Shing. Fitting ellipses to a region with application in calligraphic stroke reconstruction. In *Image Processing, 2006 IEEE International Conference on*, pages 397–400, 2006.

[39] Y. Xie and Q. Ji. A new efficient ellipse detection method. In *Pattern Recognition*, pages 957–960, 2002.

[40] L. Xu, E. Oja, and P. Kultanen. A new curve detection method: randomized hough transform (rht). *Pattern Recognition Letters*, 11(5):331–338, 1990.

[41] P. Yin. A new circle/ellipse detector using genetic algorithms. *Pattern Recognition Letters*, 20(7):731–740, 1999.

[42] B. Yuan and M. Liu. Power histogram for circle detection on images. *Pattern Recognition*, 48(10):3268–3280, 2015.

[43] H.K. Yuen, J. Illingworth, and J. Kittler. Detecting partially occluded ellipses using the hough transform. *Image and Vision Computing*, 7(1):31–37, 1989.

[44] G. Zhang, D. Jayas, and N. White. Separation of touching grain kernels in an image by ellipse fitting algorithm. *Biosystems engineering*, 92(2):135–142, 2005.

[45] S. Zhang and Z. Liu. A robust,real-time ellipse detector. *Pattern Recognition*, 38(2):273–287, 2005.